A Study on Damage Detection in Steel Structures using Changes in the Curvature of Power Spectral Density

Kitami Institute of Technology	○Student Member	Sherif Beskhyroun
Kitami Institute of Technology	Fellow	Toshiyuki Oshima
Kitami Institute of Technology	Member	Tomoyuki Yamazaki
Kitami Institute of Technology	Member	Yutaka Tsubota
Hakodate Dock Co. Ltd.		Akihiko Atsumi

1. Introduction

Civil engineering structures are not built for eternity. Service loads, environmental and accidental action may cause damage to structures. Regular inspection and condition assessment of engineering structures are necessary so that early detection of any defect can be made and the safety and reliability of the structure can be determined. Early damage detection and damage location allows maintenance and repair works to be properly programmed, thereby minimizing costs. Current damage detection methods are either visual or localized experimental methods such as acoustic or ultrasonic methods, magnet field methods, radiographs, eddy-current methods and thermal field methods. All of these experimental techniques require that the location of the damage is known a priori and that the portion of the structure being inspected is accessible. When the structural damage is small or it is in the interior of the system, it cannot be detected visually. A useful, though more elaborate, non destructive evaluation (NDE) tool is vibration monitoring. Damage or fault detection as determined by changes in the dynamic properties or response of structures is a subject that has received considerable attention in literature. The basic idea is that the occurrence of damage or loss of integrity in a structural system leads to a changed response to dynamic forces caused by changes in the dynamic properties of the structure (eigenfrequencies, modal damping rates, mode shapes and/or transfer functions). Extensive research is carried out on the development of non-destructive damage assessments methods and the translation of changes of modal characteristics in occurred damage in a structure[1-7].

In the present paper we present a practical method to detect damage and locate its position by using changes in the curvature of Power Spectral Density (PSD). First, we outline a damage detection algorithm to detect and locate damage in structures using changes in the PSD curvature. Next, we describe a steel bridge model, use the proposed algorithm and the collected data to detect damage and locate its position in the test structure. Finally, we assess the practicality of proposed algorithm by quantifying the accuracy of the obtained results from the test structure.

2. Damage detection algorithm

Denoting G_{if} the PSD magnitude at channel number i at frequency value f and $\{G_f\}$ a vector representing PSD magnitudes at all measured points at the same frequency, f. Before analyzing PSD data, the PSD data has to be first normalized. There are several approaches in which to normalize the PSD data. For this problem, the approach taken was to normalize the PSD magnitudes at each frequency with respect to the square root of the sum of squares (SRSS) as shown in the following expression

$$\{P_f\} = \frac{1}{\sqrt{\sum_{i=1}^{n} G_{if}^2}} \{G_f\} \tag{1}$$

where $\{P_f\}$ = the normalized PSD magnitudes, $\{G_f\}$ represent the original PSD magnitudes at frequency f gathered experimentally or analytically, n = the number of measured points, and G_{if} represents PSD magnitude at channel i at frequency f.

The damage index is defined as the absolute difference in PSD curvature before and after damage as follows

$$S_{if} = \left| P_{if}'' - P_{if}^{*''} \right| \tag{2}$$

where P_{if}'' and $P_{if}^{*''}$ are the second derivative of PSD magnitude at frequency f at node i corresponding to the undamaged and damaged structure, respectively. Assuming that the collection of the damage indices, S_{if}, represents a sample population of a normally distributed random variable, a normalized damage indicator is obtained as follows

$$Q_{if} = \frac{S_{if} - \overline{S_f}}{\sigma_f} \tag{3}$$

where $\overline{S_f}$ and σ_f represent the mean and standard deviation of the damage indices, respectively and defined as follows

$$\overline{S_f} = \sum_{i=1}^{n} S_{if} \Big/ n \tag{4}$$

$$\sigma_f = \sqrt{\sum_{i=1}^{n} (S_{if} - \overline{S_f})^2} \Big/ (n-1) \tag{5}$$

where n = the number of measured points.

When Q_{if} is calculated at different frequencies on the measurement range, from $F1$ to $F2$, at different nodes, from 1 to n, the maximum absolute value of Q_{if} is defined as follows

$$Q_{\max} = \max(|Q_{if}|) \tag{6}$$

where $f = F1:F2$ and $i = 1:n$

A statistical decision making procedure is employed to determine if the normalized damage index, Q_{if}, is associated with a damage location. Values of Q_{if} equal to or greater than 80% of Q_{max}, are assumed to be associated with damage locations. In order to reduce the effect of positive false readings, Q_{if} values less than 80% of Q_{max} will be removed and values greater than or equal to 80% of Q_{max} will be added over different frequencies on the measurement range from $F1$ to $F2$. In other words

$$\text{if } |Q_{if}| < (0.80 * Q_{\max}) \text{ then let } Q_{if} = 0 \text{ and } D_{if} = 0 \tag{7}$$

$$\text{if } |Q_{if}| \geq (0.80 * Q_{\max}) \text{ then let } Q_{if} = Q_{if} \text{ and } D_{if} = 1 \tag{8}$$

$$A_i = \sum_{f=F1}^{F2} |Q_{if}| \tag{9}$$

In Eqs. (7) and (8), D_{if} is used as a counter to identify the number of times damage is detected at node number i. Adding the value of D_{if} over the different frequencies gives the total number of times damage is detected at node number i on the measurement range as follows

$$O_i = \sum_{f=F1}^{F2} D_{if} \tag{10}$$

Multiplying the damage index, A_i, by the total number of times, O_i, defines the accumulated damage indicator, DI_i

$$DI_i = A_i O_i \tag{11}$$

3. Experimental setup and numerical model

In this research, a steel bridge model is examined after inducing damage with different levels to some members. The model consists of two girders and six cross beams. Each cross beam is connected to the girders with four bolts, 2 bolts in each side. The model dimensions and layout are shown in Figs. 1 and 2. The multi-layer piezoelectric actuator is used for local excitation. The main advantage of using piezoelectric actuator is that it produces vibration with different frequencies ranging from 0.1 to 400 Hz that is effective in measuring mode shapes[8),9)]. The actuator force amplitude is 0.2 kN. One accelerometer is attached to the bottom of each cross beam to measure the acceleration response in the vertical direction at the mid span of each cross beam, as shown in Fig. 2. PSD is then calculated from the acceleration data for the intact and damaged structure. Cubic polynomial is used to approximate PSD magnitude between sensors in order to create artificial degrees of freedom[5)] and to calculate the curvature of PSD data.

Four cases of damage are introduced to the specimen as follows:

Case 1: Removing one bolt from the left side of cross beam no. 10 (Fig. 3).

Case 2: Case 1 + releasing one bolt at the left side of cross beam no 10 (Fig. 3).

Case 3: Case 2 + removing one bolt at the right side of cross beam no 10 (Fig. 3).

Case 4: Removing one bolt from the left side of cross beam no. 10 and removing one bolt from the left side of cross beam no. 40.

The finite element model of the bridge model is created using Structural Analysis Program, SAP2000. Main girders and cross beams are simulated by shell elements. The FE model contains 338 shell elements and 2292 active degrees of freedom. The density of steel is assumed to be 77 kN/m3 and the modulus of elasticity of steel is assumed to be 206 GPa. The actuator excitation is simulated by a random time history signal. The random signal is defined by 10000 data points at 0.001 s increments. The excitation force is applied as a time varying concentrated vertical load on the main girder. Acceleration response in the vertical direction is measured at the mid span of each cross beam. The main objective of using the numerical data is to assess different effects rather than noise or measurement errors on the accuracy of the obtained results from the studied Damage Identification Method (DIM).

Four cases of damage are studied using the numerical data as follows:

Case 1A: Reducing the cross sectional area of one shell element at the left side of cross beam no. 10, hanning window size is 256, PSD is measured in the frequency range from 20 to 200 Hz.

Case 1B: The same as Case 1A except for the change in frequency range. PSD is measured in the frequency range from 20 to 400 Hz.

Case 1C: The same as Case 1A except for the change in window size. The window size is 512.

Case 2: Reducing the cross sectional area of one shell element at the left side of cross beam no. 20, hanning window size is 256, PSD is measured in the frequency range from 20 to 200 Hz.

4. Application of the damage identification algorithm to different damage cases

4.1 Experimental data

PSD magnitude is measured in the frequency range from 20 to 200 Hz for the intact structure and for each case of damage. Fig. 4 shows the obtained results for Case 1 of damage at cross beam no 10. Damage could be detected and

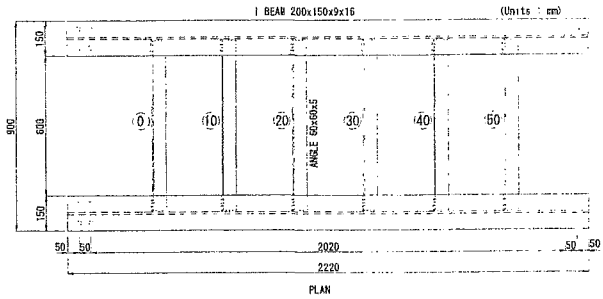

Fig. 1 Specimen dimensions

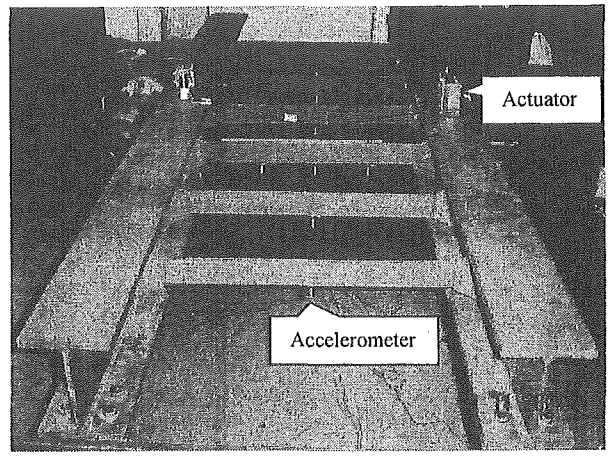

Fig. 2 Accelerometers and actuator positions

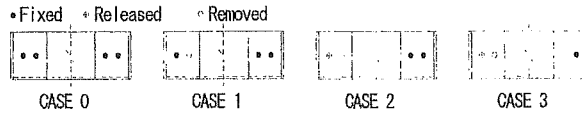

Fig. 3 Cases of damage introduced to cross beam no. 10

located accurately at node 10 with some positive false readings appeared at nodes 20, 30 and 40. The second figure shows the total number of detecting damage at each node as determined from Eq. (10). Although the number of false positive readings is big, their accumulated damage indicator values are small compared to the value at the correct position. As the damage increases in Case 2 and Case 3, the number of false positive readings decrease as can be shown clearly in Figs 4, 5 and 6. Moreover, the number of detecting the damage at the correct position increases as the damage level increases. It is noticed also that the value of accumulated damage indicator increases significantly compared to its value at the false positive readings as the level of damage increases. Fig. 7 shows the normalized damage indicator value at each node versus the frequency value at which PSD is measured; the figure is drawn for Case 3. In this figure, damage at node no 10 is detected at almost every frequency value in the measurement range from 20 to 200 Hz which ensures the existence of damage at this node. On the other hand, false positive readings appear few times at some frequency values. The best frequency range in which PSD should be used is a potential area of further research. The results obtained for Case 4 (multiple damage) is shown in Fig. 8. Both positions of damage in cross beams 10 and 40 are detected accurately. The value of accumulated damage indicator at false positions is very small compared to its value at the correct positions.

4.2 Numerical data

Since numerical data is free from noise and measurement errors, it can be used to evaluate the accuracy of the studied

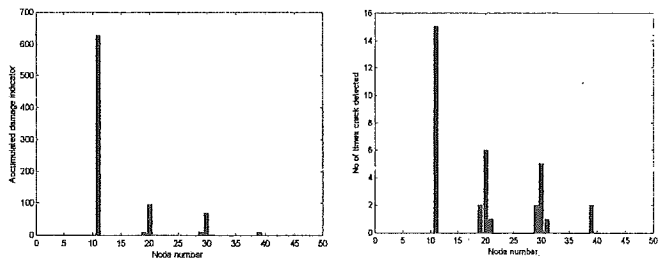

Fig. 4 DIM applied to experimental data for Case 1

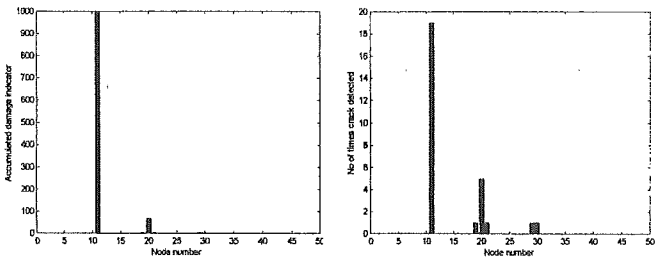

Fig. 5 DIM applied to experimental data for Case 2

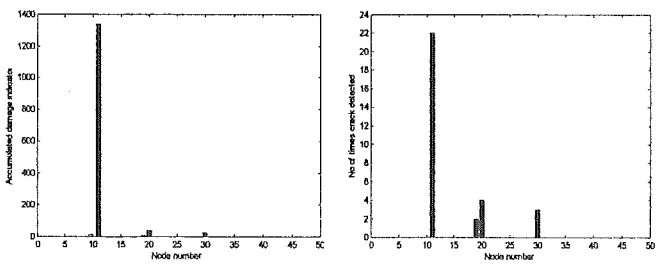

Fig. 6 DIM applied to experimental data for Case 3

damage identification method. In this section, the effect of the measurement range of PSD, window size and changing the damage location on the results will be discussed.

In Case 1A, PSD magnitude is measured in the same frequency range from 20 to 200 Hz and a hanning window size is 256 as was used for the experimental data. Damage at beam no. 10 is detected accurately as shown in Fig. 9 with a very high value of accumulated damage indicator. A number of false positive readings appeared around node 20, their accumulated damage indicator values are very small compared to the value at the correct position (node 10). Fig. 10 shows the normalized damage indicator value at each node versus the frequency value at which PSD is measured. As was noticed in the experimental data, damage at node no 10 is detected accurately at almost every frequency value and some false positive readings appear at few frequency values. The false positive readings exist here due to the accuracy of the damage identification algorithm since the data is free of noise. In Case 1B, PSD magnitude is measured in the frequency range from 20 to 400 Hz. The obtained result for this case is shown in Fig. 11. Comparing the results of Case 1A to Case 1B, the following remarks can be concluded:

1- The accumulated damage indicator value at the damage location increased significantly to the value of 15000 compared to the value of 4500, when larger measurement range was used.
2- The total number of detecting damage at the correct location increased to 79 compared to 41, when larger measurement range was used.
3- The number of false positive readings appeared at more locations in Case 1B, their accumulated damage indicator values were small in both cases.

When a wide range of frequency range is used, PSD will be measured at more frequency values, which will increase the number of times of detecting the damage and hence the value of accumulated damage indicator. On the other hand, the number of false positive readings is expected also to increase. In experimental data, some regions in the frequency range contain more noise than other regions. Therefore, wide range of measurement is recommended only if the range contains low noise. Fig. 12 shows the results of Case 1C where the window size is increased to 512. Comparing the results obtained from this case to the results obtained from Case 1A (Fig. 9), it is noticed that better results are obtained; accumulated damage indicator value and number of times of detecting the damage increased, however the number of false positive readings increased a little. The results obtained from Case 1C are very similar to the results of Case 1B. In Case 1C, a short range of measurement is used with high resolutions on the other hand, in Case 1B a wide range of measurement is used with a low resolution. The case of using wide range of measurement (from 20 to 400 Hz) and using bigger window size (512) is also studied but the results are not shown in this paper due to the limited space. In this case, the same previous remarks were also observed; accumulated damage indicator value and number of times of detecting the damage increased, and the number of false positive readings appeared at more places. The accuracy of damage identification methods based on mode shapes is sometimes reduced when the damage exist at the node of the used modes. In order to evaluate the effect of changing the damage position on the results, damage position is changed in Case 2 to node no 20. The obtained results of this case are shown in Fig. 13. The damage is indicated very accurately at node 20 and the number of false positive readings decreased compared to Case 1A (at node 10).

The accurate results obtained from the numerical data ensure the applicability of the studied damage identification method. Moreover, the numerical data can give good information about the expected results from different scenarios of damage. Numerical data can be a useful tool to determine the most effective frequency range that should be used as a measurement range for each scenario of damage.

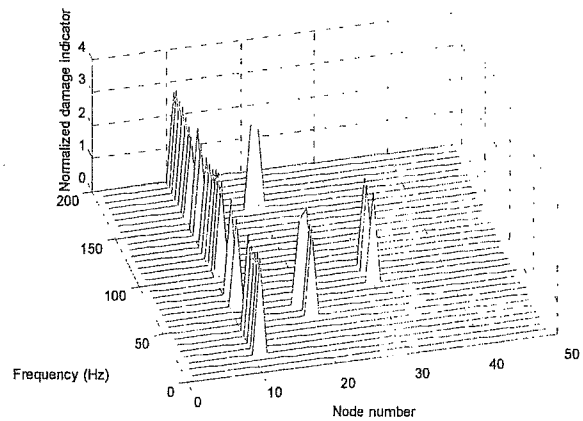

Fig. 7 DIM applied to experimental data for Case 3, normalized damage indicator value at each frequency.

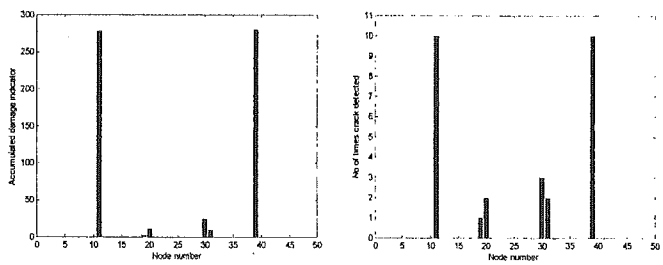

Fig. 8 DIM applied to experimental data for Case 4

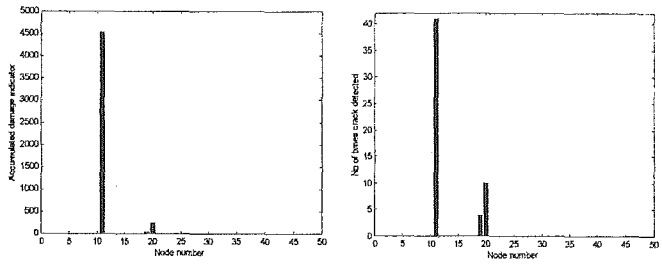

Fig. 9 DIM applied to numerical data for Case 1A

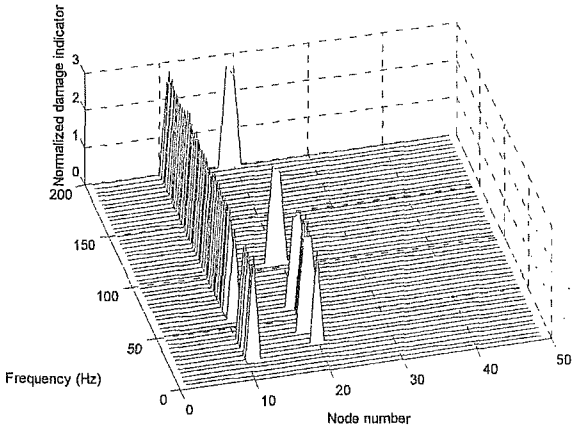

Fig. 10 DIM applied to numerical data for Case 1A, normalized damage indicator value at each frequency.

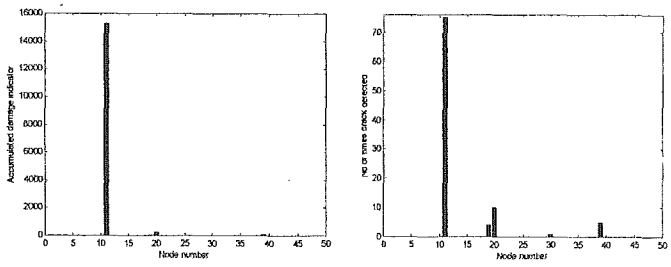

Fig. 11 DIM applied to numerical data for Case 1B

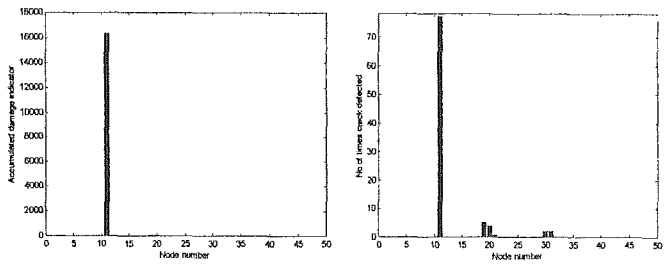

Fig. 12 DIM applied to numerical data for Case 1C

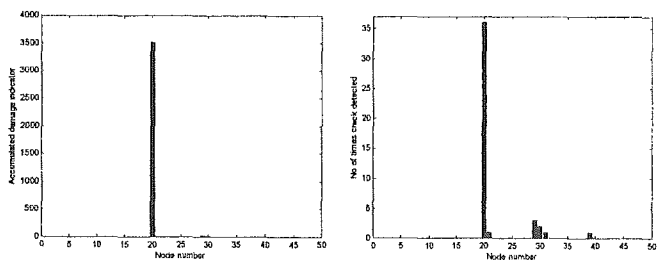

Fig. 13 DIM applied to numerical data for Case 2

Conclusion

(1) Changes in the curvature of PSD magnitude due to the presence of structural damage, represented here in a steel bridge model, have been investigated. The results of the steel bridge model demonstrate the usefulness of the changes in the curvature of PSD magnitude as a diagnostic parameter in detecting and locating damage in the cross beams of the bridge model.

(2) The proposed algorithm showed good results in detecting and locating damage in different places and for single and multiple-damage.

(3) In this study, all damage results that have been identified by the proposed algorithm were determined without use of the measured input to the structure since PSD is measured from the acceleration response of the structure. Therefore, the algorithm can be used for continuous health monitoring of structures using ambient vibration as an excitation force.

(4) Damage identification method studied here has shown better results when wide range of measuring PSD was used. On the other hand, choosing the frequency range in which PSD should be measured in the experimental data, that usually contains noise and measurement errors, needs further investigation.

Acknowledgement

This research is supported by the Grant-in-Aids for Scientific Research, Ministry of Education. The authors wish to thank for this support. Special thanks to Dr. Mikami, Mr. Wakasugi of Hakodate Dock Co. Ltd. and Mr. Kumagai for their contributions to the experimental study.

References

1) Johan Maeck, *Damage Assessment of Civil Engineering Structures by Vibration Monitoring*, Ph.D. thesis, Katholieke Universiteit Leuven, 2003.
2) R. P. C. Sampaio, N. M. M. Maia and J. M. M. Silva, *Damage detection using the frequency response-function curvature method*, Journal of Sound and Vibration 226(5), 1029-1042, 1999.
3) Peeters B., Maeck J. and De Roeck G., Vibration-based damage detection in civil engineering: excitation sources and temperature effects, *Smart Mater. Struct.* 10 pp.518-527, 2001.
4) Doebling S. W., C. R. Farrar, M. B. Prime, and D. W. Shevitz, *Damage Identification and Health Monitoring of Structural and Mechanical Systems from Changes in their Vibration Characteristics*, A Literature Review, Los Alamos National Laboratory Report, LA-13070- MS, 1996.
5) Farrar C. R. and D. A. Jauregui, *Damage Detection Algorithms Applied to Experimental and Numerical Model Data from the I-40 Bridge*, Los Alamos National Laboratory Report, LA-12979-MS, 1996.
6) Farrar C. R. and D. A. Jauregui, Comparative study of damage identification algorithms applied to a bridge: I. Experiment, *Smart Mater. Struct.* 7 pp.704-719, 1998.
7) Farrar, C. R. and D. A. Jauregui, Comparative study of damage identification algorithms applied to a bridge: II. Numerical study, *Smart Mater. Struct.* 7 pp.704-719, 1998.
8) Oshima T. et al., Study on damage evaluation of joint in steel member by using local vibration excitation (In Japanese), *Journal of Applied Mechanics*, Vol.5, pp.837-846, 2002.
9) Beskhyroun S., Oshima T. et al., Damage detection and localization on structural connections using vibration based damage identification methods, *Journal of Applied Mechanics*, Vol.6, pp.1055-1064, 2003.